

## **Analysis of Adhesive Bonded Single Lap Joints in Hybrid Composites Subjected to Transverse Load With S-S End Conditions**

**G.N. Rao<sup>1</sup>, M.V. Rao<sup>1</sup>, K.M. Rao<sup>2</sup>, V.R. Raju<sup>3</sup>, V.B.K. Murthy<sup>4</sup>  
and V.V.S. Raju<sup>4</sup>**

<sup>1</sup>*Mech. Engg. Dept., Bapatla Engineering College, Bapatla, A.P, India.  
Email: mvr2007rao@rediffmail.com*

<sup>2</sup>*K.L. College of Engineering, vaddeswaram, A.P., India.*

<sup>3</sup>*J.N.T. University, Vizayanagaram, A.P., India.*

<sup>4</sup>*Mech. Engg. Dept, P. V. P. Siddhartha Institute of Technology,  
Vijayawada, A.P, India.*

### **Abstract**

The present investigation deals with the static analysis of adhesive bonded single lap joint in Hybrid composite using three-dimensional theory of elasticity based finite element method. The finite element model is validated with the available results in the literature for the longitudinal loading of a single lap joint (SLJ) made of specially orthotropic laminates and is extended for the analysis of Hybrid (FRP-Steel) single lap joint subjected to transverse loads. The out-of-plane normal and shear stresses are computed at the interfaces of the adherends and adhesive, and at mid surface of the adhesive. The results of the present analysis reveals that the three-dimensional stress analysis is required for the analysis of adhesive bonded single lap joint in Hybrid (FRP-Steel) composites.

**Key words:** SLJ, FEM, FRP, Inter-laminar stresses

### **Introduction**

Fiber reinforced plastic (FRP) materials have proven to be very successful in structural applications. They are widely used in the aerospace, automotive and marine industries. FRP materials or composites behave differently than typical metals such as steel or aluminum. A typical composite contains layers of aligned fibers oriented at different angles held together by a resin matrix, giving high strength and stiffness in

different directions. This anisotropy can cause difficulties when joining two parts together, especially if the two pieces have different stiffness and strength characteristics. The joint can potentially become the weakest link in the structure due to the large amount of load it must transfer. There are a wide variety of ways to join different parts together. Two major methods include mechanical fastening and adhesive bonding. Adhesive bonding of structures has significant advantages over conventional fastening systems. Bonded joints are considerably more fatigue resistant than mechanically fastened structures because of the absence of stress concentrations that occur at fasteners. Joints may be lighter due to the absence of fastener hardware. A major advantage of adhesive bonds is that adhesive bonds may be designed and made in such a way that they can be stronger than the ultimate strength of many metals in common use for aircraft construction.

The stresses induced at the interfaces of the adherends and adhesive play an important role in the design of adhesive bonded joints in FRP composites. Hence, these stresses are required to be analyzed most accurately.

In 1938, Volkersen [1] first proposed a simple shear lag model for mechanical joints with many fasteners, and later on, this model was adopted for adhesively bonded lap joints with the assumption that the adherends are in tension and adhesive is in shear only and both stresses are constant across the thickness. In 1944, Goland and Reissner [2] took into consideration the effects of the adherends bending and the peel stress, as well as the shear stress, in the adhesive layer in a single lap joint. Subsequent efforts by Oplinger [3] suggested the corrections to the Goland and Reissner solution by using a layered beam theory instead of classical homogeneous beam model for single lap joints. The corrections in the shear lag model, or Volkersen solution, include works by Hart-Smith [4,5] and Tsai et.al [6]. Hart-Smith [4,5] modified the shear lag model to include the adhesive plasticity. Tsai et.al [6] provided a correction to the shear lag model with the assumption that the shear stress is linear through the adherends. The analysis of Klarbring and Movchan [7] involved mathematically modeling the adhesive joint using an asymptotic approach. Kim and Kedward [8] used finite difference method for the analysis of adhesively bonded joints. Penado and Dropek [9] and Tessler et.al [10] used finite element method for the analysis of adhesively bonded joints.

Adams and Peppiatt [11] analyzed a bonded joint using a two dimensional linear elastic finite element method with plane strain assumption. Examples of finite element investigations of adhesively bonded composite joints include Kairouz and Matthews [12], Tong [13], Li et al. [14]. Delale et al. [15] developed a closed-form solution for lap-shear joints with orthotropic adherends using classical plate theory. Mortensen [16] presented a unified analytical approach to analyze an array of common bonded joint configurations for more general loading conditions. Panigrahi and Pradhan [17] studied; a single lap joint with the adherends made of specially orthotropic laminates for the evaluation of the tri-axial stress field using finite element analysis and proved the necessity of three-dimensional stress analysis of single lap joint.

The objective of the present paper is to extend the three-dimensional stress analysis of Panigrahi and Pradhan [17] for the analysis of Hybrid (FRP-Steel) single lap joint with adherends made of generally orthotropic laminate and steel plate. The

analysis includes the evaluation of i) Inter-laminar normal stress ( $\sigma_{zz}$ ), ii) Inter-laminar shear stress in longitudinal plane ( $\tau_{zx}$ ) and iii) Inter-laminar shear stress in transverse plane ( $\tau_{yz}$ ) at the interfaces of the adherends and adhesive, and at the middle plane of the adhesive.

## Problem Modeling

### Geometry

The geometry of the problem used for longitudinal loading is as shown in Fig. 1. In case of transverse loading, the thickness of the adherends is increased to maintain the length-to-thickness ratio ( $s$ ) equal to 10. The thickness of the adhesive is increased proportionately with the thickness of the adherends. The in-plane dimensions for the transverse loading are same as that of longitudinal loading.

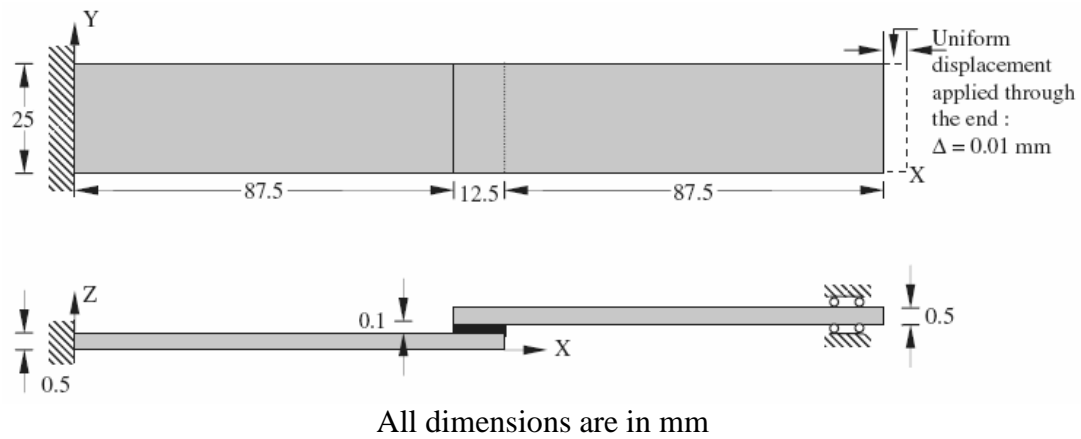


**Figure 1:** Geometry of the single lap joint.

### Finite Element Model

The finite element mesh is generated using a three-dimensional brick element 'SOLID 45' of ANSYS [18]. This element (Fig. 2) is a structural solid element designed based on three-dimensional elasticity theory and is used to model thick orthotropic solids. The element is defined by 8 nodes having three degrees of freedom per node: translations in the nodal x, y, and z directions.

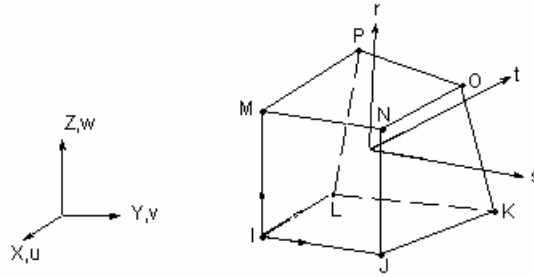


**Figure 2:** SOLID 45 Element.

### Loading

The following types of loads are applied for validation and prediction of the response of the structure for the present analysis.

- (i) A uniform longitudinal displacement of 0.01 mm for the validation purpose.
- (ii) A uniform transverse load of 1 MPa is applied for the present analysis

### Boundary Conditions

Both the ends of the joint are simply supported

### Material Properties

The following mechanical properties are taken for the analysis of joint.

#### *Epoxy (adhesive)*

$$E = 5.171 \text{ GPa}; \quad \nu = 0.35;$$

#### *Graphite-Epoxy (adherends)*

$$E_1 = 172.72 \text{ GPa}, \quad E_2 = E_3 = 6.909 \text{ GPa}$$

$$G_{12} = G_{13} = 3.45 \text{ GPa}, \quad G_{23} = 1.38 \text{ GPa}, \quad \nu_{12} = \nu_{13} = \nu_{23} = 0.25$$

#### *Steel (Top Adherend)*

$$E = 2 \text{ GPa}; \quad \nu = 0.25$$

### Laminate sequence

- (i) Two  $0^0/90^0/90^0/0^0$  laminated FRP composite plates are used as adherends for the validation of present FE model with reference [17].
- (ii) One  $+ \theta^0 / - \theta^0 / - \theta^0 / + \theta^0$  laminated FRP composite plate and One Steel Plate are used as adherends for the present analysis. The value of  $\theta$  is measured from the longitudinal direction of the structure (x-axis) and varied from  $0^0$  to  $90^0$  in steps of  $15^0$

## Results

### Validation

Fig. 3 shows the finite element mesh on the overlap region of the single lap joint. The present finite element model is validated by comparing the stresses obtained for the single lap joint of specially orthotropic laminates with the results of reference [17] for longitudinal loading. Table. 1 shows the comparison of maximum values of the stresses at the specified locations and close agreement is found. Later this model is extended for the analysis of single lap joint of generally orthotropic laminates subjected to longitudinal and transverse loading.

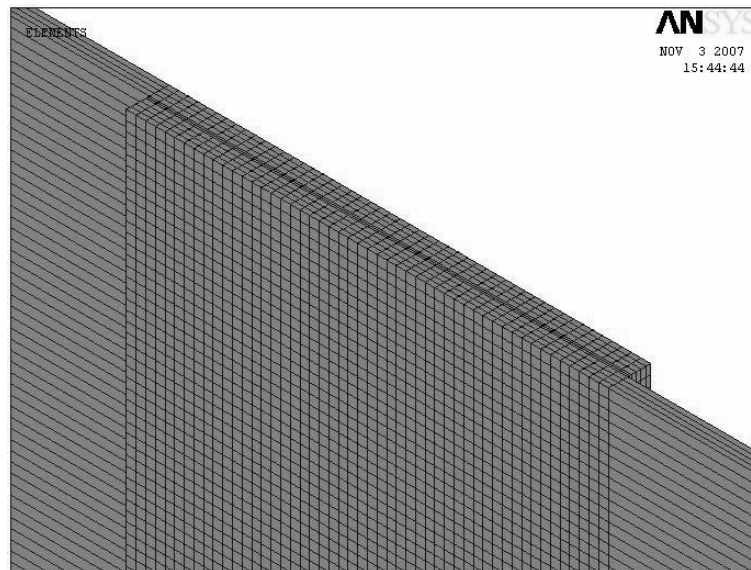


**Figure 3:** Finite element mesh on the overlap region of the single lap joint.

**Table 1:** Validation of the finite element model.

Location	$\sigma_{zz}$ (MPa)		$\tau_{yz}$ (MPa)		$\tau_{zx}$ (MPa)	
	Ref [17]	Present	Ref [17]	Present	Ref [17]	Present
Top Interface	0.40	0.41	0.08	0.14	0.39	0.40
Bottom Interface	0.39	0.39	0.08	0.13	0.38	0.39

### Variation of the stresses across the width of the laminate

One of the reasons for the variation of the stresses across the width of the laminate is due to the non-uniform arrangement of the fibers in the width direction except at  $\theta = 0^{\circ}$  and  $90^{\circ}$ . The second reason is due to the coupling between bending, shear, and extensions in the deformations of the laminates. Another reason is due to the inter-laminar effect at the free edges of the structure.

The Fig. 4 illustrates the variation of normal stress,  $\sigma_{zz}$ , across the width for several fiber angles. There is no significant variation of stress for  $\theta=0^\circ$  and  $90^\circ$  at the middle surface of joint but change in stress at the ends is observed. For  $\theta=30^\circ$ ,  $45^\circ$  and  $60^\circ$  the stress is varying non linearly with minimum value at  $y=0\text{mm}$  and maximum value at  $y=25\text{mm}$ .

Fig. 5 shows the variation of shear stress,  $\tau_{yz}$ , with  $\theta$  across the width of joint. The shear stress for  $\theta=0^\circ$  and  $90^\circ$  is negative between  $0\text{mm}$  and  $12.5\text{mm}$ , positive between  $12.5\text{mm}$  and  $25\text{mm}$  with maximum value at the ends and zero value at  $y=12.5\text{mm}$ . This stress for  $\theta=30^\circ$ ,  $45^\circ$  and  $60^\circ$  increases slightly up to  $y=18.5\text{mm}$  followed by drop in stress.

Variation of shear stress,  $\tau_{zx}$ , across width for several fiber angles is shown in Fig.6. we see that the negative shear stress for  $\theta=0^\circ$ ,  $30^\circ$ ,  $45^\circ$  and  $60^\circ$  increases rapidly up to width of  $5\text{mm}$ , after which the variation in shear stress  $\tau_{zx}$  is slow up to  $y=20\text{mm}$  followed by drop in stress. For  $\theta=90^\circ$ , there is no significant variation of stress between  $y=5\text{mm}$  and  $20\text{mm}$  followed by decrease in stress and increase in stress at both the ends is observed.

In most of the above cases, it is observed that the stresses are maximum near the ends of the plate in the width direction. This may be due to the inter-laminar effect in addition to the coupling effect. The stresses shown in Figs. 4-6 are measured at the locations where the normal and shear stresses are maximum in the bottom interface of the adherend and adhesive.

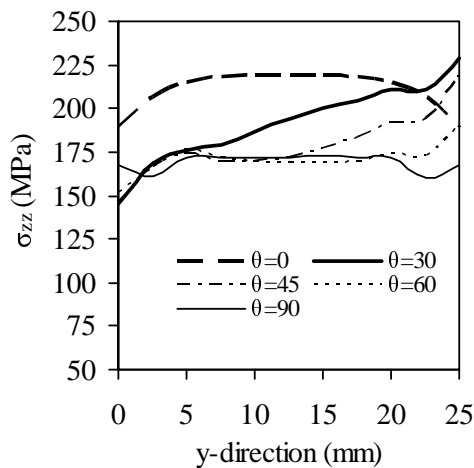


**Figure 4:** Variation of  $\sigma_{zz}$  across width.

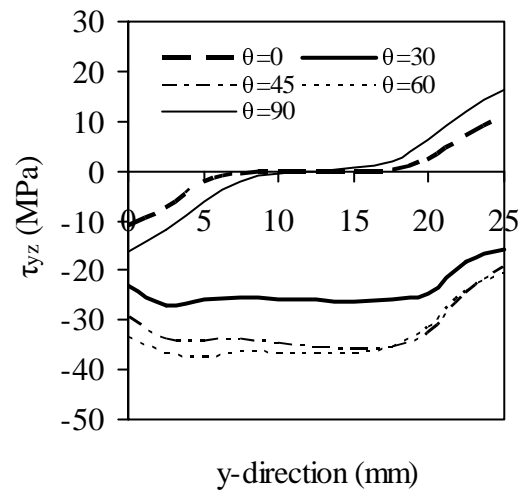


**Figure 5:** Variation of  $\tau_{yz}$  across width.

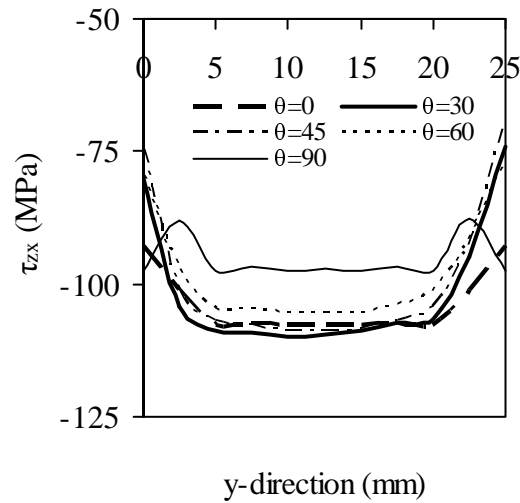


**Figure 6:** Variation of  $\tau_{zx}$  across width.

#### Variation of the maximum stresses with respect to the fiber angle $\theta$ .

Load transfer between adjacent layers in a fiber-reinforced laminate takes place by means of interlaminar stresses, such as  $\sigma_{zz}$ ,  $\tau_{zx}$ , and  $\tau_{yz}$ . The variation of these stresses with respect to the fiber angle at the interfaces of single lap joint is due to the following reasons.

- The mismatch in the poisson's ratios at the inter-faces of adherends and adhesive results in the variation of inter-layer stresses with respect to the fiber angle. When the fiber angle,  $\theta=0^0$ , the mismatch in the poisson's ratios of adhesive and adherend materials is maximum. As the fiber angle increases, the poisson's ratio of the adherend increases up to certain value of  $\theta$  and later decreases, as a result the mismatch in poisson's ratio decreases up to certain value of  $\theta$  and later increases. Due to this effect, the inter-layer stresses may decrease up to certain value of  $\theta$  and later increase.
- The second reason for the variation of inter-layer stresses with respect to fiber angle is due to the effect of coefficients of mutual influences or due to the coupling between shear, extension and bending deformations of the laminate. This effect causes for the increase in inter-layer stresses up to certain value of  $\theta$  and later decrease.

As the force transmission takes place through the interlaminar stresses from the adherend to adhesive, the stresses at the mid plane of adhesive will also be affected by the fiber angle. Therefore the variation of stresses with respect to fiber angle  $\theta$  on various interfaces is due to the resultant effect of above given reasons.

Fig. 7 depicts the variation of normal stress,  $\sigma_{zz}$ , with  $\theta$  on various surfaces. The variation of this stress on all the surfaces is zig-zag and this stress shows the largest response on bottom interface at all the fiber angles.

Fig.8 illustrates the variation of shear stress,  $\tau_{yz}$ , on several surfaces. This stress on top, mid surface and bottom interface increases up to  $45^0$ ,  $45^0$  and  $58^0$  respectively and

declines later with increase of  $\theta$ . According to Fig.9 it can be observed that the slight variation of shear stress,  $\tau_{zx}$ , on all the surfaces with increase of fiber angle  $\theta$ .

The variation of transverse deflection 'w' with fiber angle  $\theta$  is shown in Fig.10. The deflection increases gradually up to  $90^\circ$  with minimum value at  $\theta=0^\circ$  and maximum at  $\theta=90^\circ$ . The factors influencing the deflection are variation of stiffness and mutual influence with  $\theta$ .

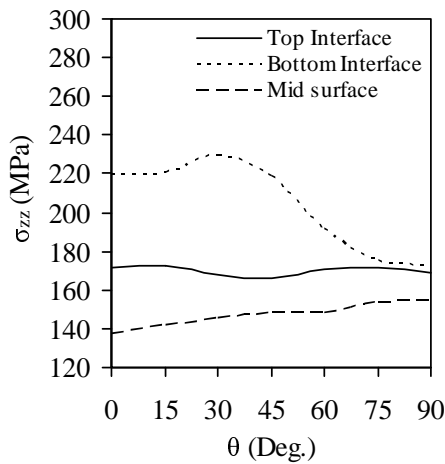


Figure 7: Variation of  $\sigma_{zz}$  with  $\theta$ .

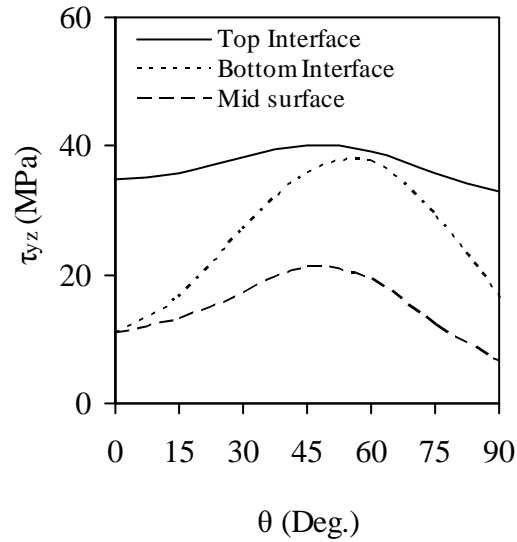


Figure 8: Variation of  $\tau_{yz}$  with  $\theta$ .

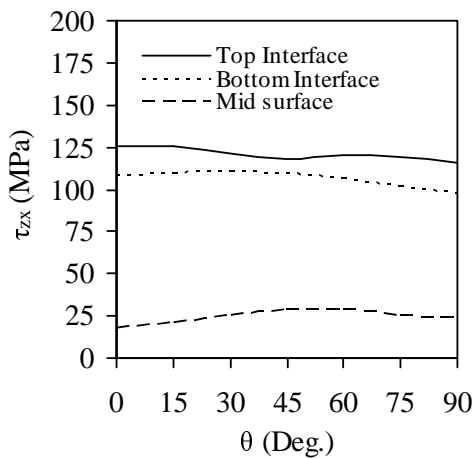


Figure 9: Variation of  $\tau_{zx}$  with  $\theta$ .

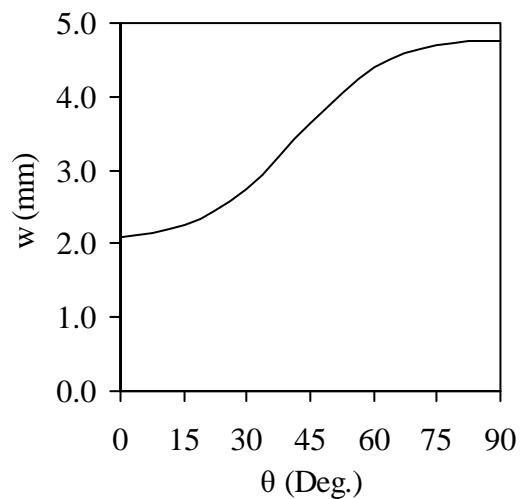


Figure 10: Variation of 'w' with  $\theta$ .

## Conclusions

Three-dimensional finite element analysis has been taken up for the evaluation of the inter-laminar stresses at the interfaces of the adherends and adhesive, and the out-of-plane stresses at the middle surface of Hybrid (FRP-Steel) single lap joint subjected to transverse loads. The following conclusions are drawn:

- Variation of the stresses in the width direction is significant and therefore three-dimensional analysis is necessary.
- The out of plane normal stress is found maximum on bottom interface for S-S end conditions. Maximum peel stress is noticed at lower fiber angles, therefore while selecting the stacking sequence for this end condition higher fiber angles are suggested to prevent the failure.
- In case of transverse loading the maximum values of inter-laminar normal stress is more followed by the inter-laminar shear stress  $\tau_{zx}$ .
- It is also observed that the coupling effect in the laminate influences the deflection and stresses, and causing for the increase in their magnitudes up to some value of fiber angle and then decreasing of the values later.

## References

- [1] Volkersen, O., 1938, "Die Niekraftverteilung in Zugbeanspruchten mit Konstanten Laschenquerschnitten. Luftfahrtforschung", 15, pp. 41–47.
- [2] Goland, M. and Reissner, E., 1944, "The Stresses in Cemented Joints", ASME Trans., Journal of Applied Mechanics, 11, pp. 17–27.
- [3] Oplinger, D. W., 1991, "A Layered Beam Theory for Single Lap Joints", Army Materials Technology Laboratory Report, MTL TR91–23.
- [4] Hart-Smith, L. J., 1973, "Adhesive-Bonded Single Lap Joints", NASA-CR-112236.
- [5] Hart-Smith, L. J., 1973, "Adhesive-bonded Double Lap Joints", NASA-CR-112235.
- [6] Tsai, M. Y., Oplinger, D. W. and Morton, J., 1998, "Improved Theoretical Solutions for Adhesive Lap Joints", Int. Journal of Solids Structures, 35(13), pp.1163–1185.
- [7] Klarbring, A. and Movchan A.B., 1988, "Asymptotic modeling of adhesive joints", Mechanics of materials, 28, pp.137-145.
- [8] Kim H. and Kedward K., 2001, "Stress analysis of adhesively bonded joints under in plane shear loading", J. Adhesion, 76, pp.1-36
- [9] Penado F.E. and Dropek R.K., 1990, "Numerical design and analysis", Engineered materials Hand book, 3, Adhesives and Sealants, ASM International.
- [10] Tessler, A., Dambach M.L. and Oplinger D. W., 2000, "Efficient adaptive mesh refinement modeling of adhesive joints", presented at the work shop on bonded joints and assemblies in aircraft, ASTM/ASC, Texas A&M
- [11] Adams, R. D. and Peppiatt, N. A., 1974, "Stress Analysis of Adhesively Bonded Lap Joints", Journal of Strain Analysis, 9, pp.185–196.

- [12] Kairouz, K. C. and Matthews, F. L., 1993, “Strength and Failure Modes of Bonded Single Lap Joints between Cross-Ply Adherends”, *Composites*, 24(6), pp.475–484.
- [13] Tong, L. and Steven, G. P., 1999, “Analysis and Design of Structural Bonded Joints”, Kluwer Academic Publishers.
- [14] Li, Gang and Lee-Sullivan, Pearl, 2001, “Finite Element and Experimental Studies on Single-lap Balanced Joints in Tension”, *Int. Journal of Adhesion and Adhesives*, 21(3), pp. 211–220.
- [15] Delale, F., Erdogan, F. and Aydinoglu, M. N., 1982, “Stresses in Adhesively Bonded Joints: A Closed-form Solution”, *Journal of Composite Materials*, 15, pp.249–271.
- [16] Mortensen, F. and Thomsen, O. T., 2002, “Analysis of Adhesive Bonded Joints: A Unified Approach”, *Composite Science and Technology*, 62(7–8), pp.1011–1031.
- [17] Panigrahi, S. K. and Pradhan, B., 2007, “Three dimensional Failure analysis and damage Propagation behavior of Adhesively bonded Single lap joints in laminated FRP Composites”, *Journal of Reinforced plastics and Composites*, 26(2), pp.183-201.
- [18] ANSYS reference manuals (2006).